Journal of Zhejiang University SCIENCE A
ISSN 1673-565X (Print); ISSN 1862-1775 (Online)
www.zju.edu.cn/jzus; www.springerlink.com
E-mail: jzus@zju.edu.cn

On the vein-stiffening membrane structure of a dragonfly hind wing*

Zhong-xue LI†1, Wei SHEN[1], Gen-shu TONG[1], Jia-meng TIAN[1], Loc VU-QUOC[2]

([1]*Institute of Structural Engineering, Zhejiang University, Hangzhou 310058, China*)

([2]*Department of Mechanical and Aerospace Engineering, University of Florida, Gainesville, FL 32611, USA*)

†E-mail: lizx19993@zju.edu.cn

Received Mar. 21, 2008; Revision accepted Aug. 22, 2008; Crosschecked Nov. 10, 2008

Abstract: Aiming at exploring the excellent structural performance of the vein-stiffening membrane structure of dragonfly hind wings, we analyzed two planar computational models and three 3D computational models with cambered corrugation based on the finite element method. It is shown that the vein size in different zones is proportional to the magnitude of the vein internal force when the wing structure is subjected to uniform out-of-plane transverse loading. The membrane contributes little to the flexural stiffness of the planar wing models, while exerting an immense impact upon the stiffness of the 3D wing models with cambered corrugation. If a lumped mass of 10% of the wing is fixed on the leading edge close to the wing tip, the wing fundamental frequency decreases by 10.7%~13.2%; if a lumped mass is connected to the wing via multiple springs, the wing fundamental frequency decreases by 16.0%~18.0%. Such decrease in fundamental frequency explains the special function of the wing pterostigma in alleviating the wing quivering effect. These particular features of dragonfly wings can be mimicked in the design of new-style reticulately stiffening thin-walled roof systems and flapping wings in novel intelligent aerial vehicles.

Key words: Dragonfly wing, Venation pattern, Wing membrane, Pterostigma, Bionics, Quivering effect
doi:10.1631/jzus.A0820211 **Document code:** A **CLC number:** TH113; TH161

INTRODUCTION

Most existing species survive from long-term evolution and natural selection, in which the fittest species continue to thrive on, while inferior ones die out. Such natural selection promotes species that adapt well to the often demanding environment of nature; and indeed most of these surviving species would have optimized structures, functions, shapes and forms. Humans should endeavor to understand and learn from nature, and then use strengths of the surviving species to ameliorate their own lives. Bionics has found many applications in engineering. For example, certain grass leaves curl up into shell-like shapes, and possess nearly perfect stability and elegant form. Enlightened from the understanding of such natural structures, we have designed and built thin-walled shell structures in large-span roof systems (Isler, 1986; Holgate, 1990). By modeling after the cobweb, architects invented economic cable domes and tented structural systems (Kawaguchi *et al.*, 1999; Liddell and Miller, 1999; Fest *et al.*, 2003; Sun and Zhang, 2005; Feng *et al*., 2007; Zhang *et al.*, 2007). The shape-forming and stiffness-adjusting mechanisms of a cell through its inner filled liquid have inspired some air-supported/liquid-supported inflatable structural systems (Schlaich *et al.*, 1994; Bradshaw *et al.*, 2002). By systematically studying birds and imitating their gliding flight, the Wright brothers invented the first engine-powered airplane (Norberg, 2002; Somervill, 2005). The pterostigma of an insect wing, which functions as a wing pitch regulator during flight, can raise the critical gliding

* Project supported by the National Natural Science Foundation of China (No. 50408022), the Visiting Scholarship from the Future Academic Star Project of Zhejiang University, and the Scientific Research Foundation for the Returned Overseas Chinese Scholars, MOE and Zhejiang Province, China

speed (at which self-excited vibrations set in) by 10% to 25% in a dragonfly (Norberg R.A., 1972; Wootton, 1990; Ellington, 1999; Dudley, 2000; Norberg U.M.L., 2002). Similarly, a steel or lead bar attached along the blade span, at or near the profile nose of helicopters and other aircrafts (Shapiro, 1955) can preclude the highly destructive rotor blade flutter and wing flutter. By imitating animals' walking, running, flying, swimming and other movements, humans have developed a number of intelligent robots and insect-like walking machines (Dillmann *et al.*, 2005). Compared with traditional tension membrane structures, a dragonfly wing is superior in that its vein-stiffening membrane structure provides greater structural stability with the least possible material expenditure. Since the wing membrane part has small flexural stiffness, if such part being used to replace the membrane in its traditional tension membrane structure, then some technical complexity, such as membrane cutting pattern and form finding in construction (Liddell and Miller, 1999; Zhang and Zhang, 2000; Fest *et al.*, 2003; Sun and Zhang, 2005; Zhang *et al.*, 2007), could be avoided. These merits can be exploited in the bionic design of new-style reticulately stiffening thin-walled roof systems (Shen, 2006; Zhang, 2007). On the other hand, dragonfly wings are highly specialized flight organs, adapted to cope with versatile, maneuverable, multi-speed flight with the least energy-consumption (Wootton *et al*., 1998). The cambered corrugation in the wings can create a more suitable lift-drag-relationship at gliding/flapping flights. Thus it is advantageous to apply the special characteristics of dragonfly wing structures to the design of the flapping wings of novel intelligent aircrafts (Ellington, 1999; Shyy *et al.*, 1999; Norberg U.M.L., 2002; Li and Zheng, 2005).

A dragonfly can perform various swift and highly maneuverable flights with its flapping wings, as a result of the highly functional and largely optimized mechanical constructions of dragonfly wings. The unique structure of dragonfly wings has become a research focus. For example, Zeng *et al.*(1996) measured the thickness and shape of dragonfly wings and Sudo *et al.*(2000) checked the surface roughness of dragonfly wings. Okamoto *et al.*(1996) characterized the effects of camber, thickness, sharpness of the leading edge and surface roughness on the aerodynamic characteristics of dragonfly wings in the flow field. Combes and Daniel (2003a; 2003b) studied the relationship between the venation pattern and the wing flexibility by measuring the displacement along the wing in response to a point force. Sunada *et al.*(1998) investigated the effect of wing corrugation on the torsional deformation of dragonfly wings. Kesel *et al.*(1998) developed several finite element models of a dragonfly wing to characterize the quality of material distribution. Norberg R.A.(1972) found that the pterostigma of dragonfly wings usually has an optimal position at the leading edge of the wing (i.e., near the wing tip), helps to alleviate the wing quivering and makes the wing beat more efficient. In the present study, unlike the previous works that already focused on the measurement of wing shapes, thickness, roughness, venation pattern, pterostigma mass of dragonfly wings, we are aiming at exploring the structural performance of the vein-stiffening membrane structure of a dragonfly wing and the function of the wing pterostigma in alleviating the quivering effect of a light-weight wing structure. In particular, its application in the design of new-style reticulately stiffening thin-walled structural systems (Shen, 2006) and the flapping wings of a novel intelligent aircraft (Li and Zheng, 2005) will be examined.

It is necessary to employ beam and thin shell elements simultaneously or to develop some super-elements consisting of multiple beam and shell elements in the modeling of vein-stiffening membrane structure of a dragonfly wing, while satisfying the compatibility between the deformed beam and curved shell elements to ensure computational efficiency and accuracy. There already exist many beam and shell elements (Ahmad *et al.*, 1970; Cook, 1981; Simo and Vu-Quoc, 1986; Ibrahimbegovic, 1995; Zhang and Cheung, 2003; Tang and Tan, 2004; Izzuddin, 2005; Zhang and Kim, 2005; Li, 2007a; 2007b; Li and Vu-Quoc, 2007; Li *et al.*, 2008) meeting this requirement. In this paper, the Beam 189 element (a 3-node quadratic beam element based on Timoshenko beam theory, which has 6 degrees of freedom of 3 translations and 3 rotations at each node and is suitable for analyzing slender to moderately stubby/thick beam structures) and the Shell 93 element (a quadratic curved shell element with 6 degrees of freedom including 3 translations and 3 rotations at each node) in ANSYS 9.0 are employed in modeling the veins and the membrane, respectively.

CONFIGURATION OF A DRAGONFLY HIND WING

Dragonflies (*Pantala flavescens*) used in sample tests were captured in early September, 2005 at Huapu Garden of Hangzhou, and the tests were fulfilled on the same day to keep all the samples fresh. All tests were carried out in the Biological Microstructure Lab of Zhejiang University, Hangzhou. The digital image of the dragonfly hind wing was achieved by using a high-resolution scanner (Fig.1).

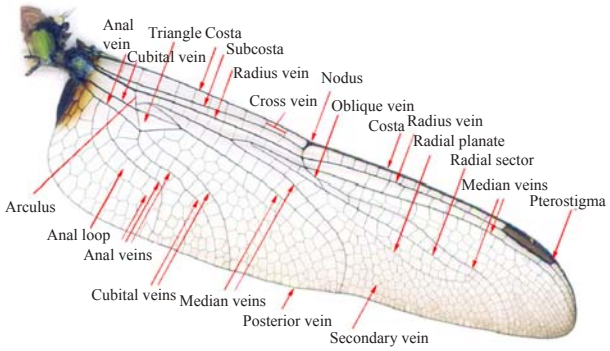

Fig.1 Image of a dragonfly hind wing

The wing structure of a dragonfly *Pantala flavescens* (Fig.1), very delicate and versatile, consists of transparent membrane pieces and tube-like veins of different sizes. The membrane seems to be extremely thin and flexible but results in a much stiffer, light-weight structure after being strengthened by the reticulate veins. The major frame (Figs.1 and 2) of the wing structure is composed of much stiffer costa, subcosta, radial veins, median veins, cubital veins, posterior vein, and part of cross veins, etc. In addition, it is reinforced further by secondary veins (Fig.1) and membrane pieces. Among unique features of the venation pattern, the vein grids close to the wing base and the leading edge are sparse and the vein sizes are much thicker, while the grids near the wing tip and the trailing edge become very dense and the veins become thinner. In addition, the grid shapes, varying in different zones and being very irregular, include trigon, tetragon, pentagon, hexagon and heptagon, etc. In the leading edge near the wing tip, there is a fuscous pterostigma, and in the middle of the leading edge there exists a nodus, where the local structures can rotate relatively.

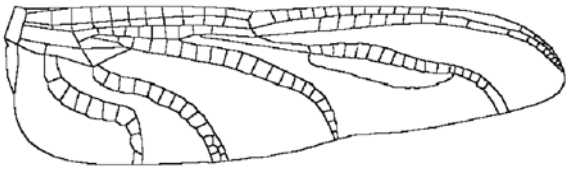

Fig.2 Major frame of a dragonfly hind wing

The unique structure of a dragonfly wing has been evolving more than three hundred million years, and consequently its structural form, performance and function are optimized systematically. Different from general membranes, the wing membrane is of small flexural stiffness, whereas the veins varies greatly in stiffness; the costa, subcosta, radial veins, median veins, cubital veins, part of cross veins and posterior vein are much stiffer yet with enough flexibility, and by contrast the other veins are much more flexible.

The dragonfly wing features a number of unique microstructures and configurations, all contributing to special functions of a wing, respectively, but difficult to be observed with unaided eyes. Thus an optical microscope and a scanning electron microscope with special cameras were utilized to take high-resolution local photographs of the wing microstructures and configurations.

Firstly, several splices were cut out from the hind wing close to the zones of the mid-span, the nodus and the pterostigma in sequence, then glued respectively to a small test-bed, and coated with platinum in an ion sputterer (IB-5 gold sputterer, Giko, Japan). By focusing on the interesting zones, a series of high-resolution photographs were taken. In Fig.3, the junction between a vein and two pieces of membranes is disclosed, and the vein has a tube-like structure. Several veins integrated with one piece of membrane form a fundamental cell of the wing structure (Fig.1); on the vein, there are many ear-like outshoots (Fig.3) in different sizes.

The microscopic photo of a pterostigma cross-section was achieved by using a scanning electron microscope (Fig.4). It is shown that the pterostigma is hollow, and has a very special configuration.

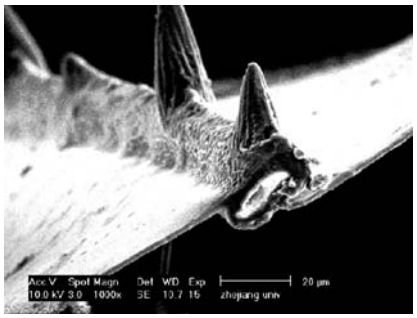

Fig.3 Junction of the vein and membrane pieces

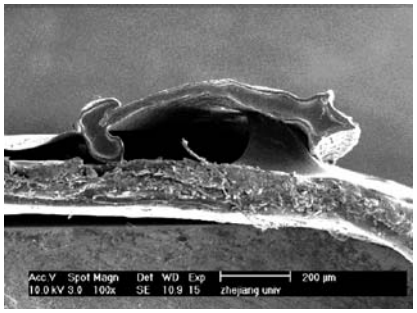

Fig.4 Microscopic cross-section of a pterostigma

As disclosed in the photographs of a wing nodus (Fig.5) and the cross-section close to the nodus (Fig.6), the structures beside the nodus are separated by a short gap adjacent to the ends of the costa and subcosta.

Fig.5 Nodus of a dragonfly hind wing

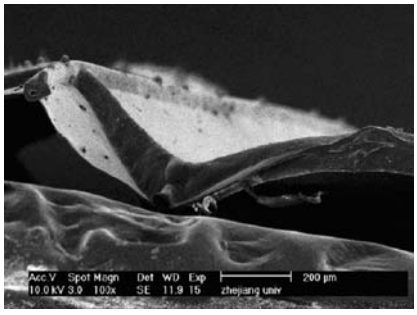

Fig.6 Microscopic photograph of a nodus cross-section

VENATION PATTERN AND VEIN SIZES VARIATION

To obtain the geometric parameters of the hind wing as accurate as possible, all the veins in the wing photo were traced directly in an AUTOCAD environment, then the coordinates of all joints of the wing were achieved from the traced figure; accordingly, the geometries of the computational models are very close to those of the projective geometry of a real hind wing (Fig.7). The traced figure is simply planar, unable to reflect the structural performance of the wing structure with cambered corrugation, so it is necessary to develop wing models with cambered corrugation from the planar figure.

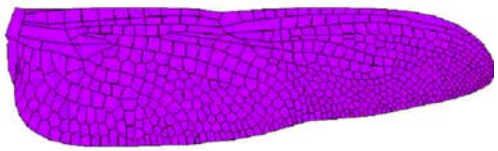

Fig.7 Planar computational model of dragonfly hind wing

In the morphological measurement of a dragonfly hind wing, Okamoto *et al.*(1996) fixed the wing with resin and sliced it transversely into several elements and then used a microscope to achieve the photograph of each cross-section (cross-sections 1, 2, 3, 4 in Fig.8). It was shown that the dragonfly wing had a 3D structure with cambered corrugation (Fig.8).

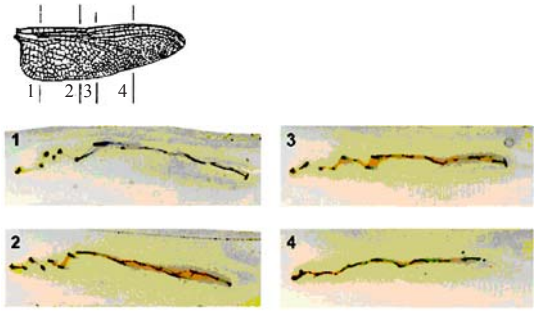

Fig.8 Cross-sections of a dragonfly hind wing (Okamoto *et al.*, 1996)

In elucidating the optimization of the venation pattern and vein sizes variation of a dragonfly hind wing, four computational models were proposed. Based on the planar model of the hind wing (Fig.7), and referred to the photograph in Fig.1 and those (Fig.8) from Okamoto *et al.*(1996), two 3D

computational models with cambered corrugation (Fig.9) were constructed by elevating the out-of-plane coordinates of certain major veins and reshaping other veins and membrane through interpolation.

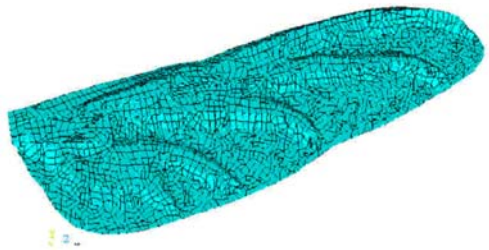

Fig.9 Meshed 3D model with cambered corrugation

Model I is a planar one (Fig.10), where the chitins of the veins and membrane are idealized as isotropic material with Young's modulus of E=6.1×10^9 N/m^2 and Poisson's ratio of 0.25 (Kesel *et al.*, 1998). All the veins are modeled using tube-like beams with the same diameter (D=0.135 mm) and thickness (t=0.025 mm); the membrane thickness in the basal zone is assumed to be 0.012 mm, and in the remaining zone 0.004 mm.

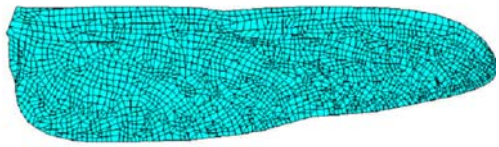

Fig.10 Meshed planar model

Model II is also a planar one (Fig.10). Referred to Fig.1, the veins are divided into ten groups with different diameters and thickness values (Table 1), while the membrane thickness and the material properties of Model II are the same as those of Model I.

Model III is a 3D model with cambered corrugation (Fig.9), where the maximum out-of-plane coordinates of the joints on the subcosta are 1 mm, and the maximum out-of-plane coordinates of the joints on median veins, radial veins and cubital veins are 0.5 mm. This spatial model is rebuilt from the planar model in Fig.7 by adjusting the out-of-plane coordinates of all joints on part of the major veins, then reshaping these veins, the rest veins and membrane through interpolation. The vein diameter and thickness, the membrane thickness of Model III, and their material properties are the same as those of Model I.

Model IV has a 3D geometry with cambered corrugation as Model III, while its vein sizes and membrane thickness are the same as Model II (Table 1), its material properties are the same as those of Models I~III.

Table 1 Vein diameters and thickness of Model II

Group	Vein diameter (mm)	Vein thickness (mm)
1	0.106	0.015
2	0.136	0.025
3	0.146	0.030
4	0.174	0.030
5	0.217	0.040
6	0.260	0.040
7	0.271	0.060
8	0.466	0.060
9	0.300	0.050
10	0.304	0.050

ANSYS 9.0 was utilized to solve these models of a dragonfly hind wing, and all models were assumed to be fully clamped along the wing root (the raised edges on the left sides of Models I~IV). Considering that most of the wing veins are curved and feature little flexural stiffness, and that the membrane is flexible but typical of small flexural stiffness, Beam 189 (Simo and Vu-Quoc, 1986; Ibrahimbegovic, 1995; Mcrobie and Lasenby, 1999) was used in modeling of the veins, and Shell 93 (Ahmad *et al.*, 1970; Cook, 1981) was adopted in modeling of the membrane, accordingly, all elements modeling of the veins and the membrane can work compatibly at a deformed state.

The mass of the present dragonfly hind wing is M=3.77×10^{-6} kg; the density of the wing material is ρ=2.86×10^2 kg/m^3; the wing length is 5×10^{-2} m, and its width is 1.43×10^{-2} m.

Under uniform out-of-plane transverse follower loading q=2 N/m^2 (downward loading, about a half of the distributed deadweight of the dragonfly wing), the distribution of the axial stresses in the veins of Models I~IV was depicted in Figs.11a~11d, and the maxima of vein axial stresses were presented in Table 2.

In Model I, the axial stresses in the veins close to the wing base and the leading edge, and in the posterior vein are much greater, while the stresses in the veins close to the wingtip and in the secondary veins are smaller (Fig.11a and Table 2). This is coincident with the sizes of the veins in different zones.

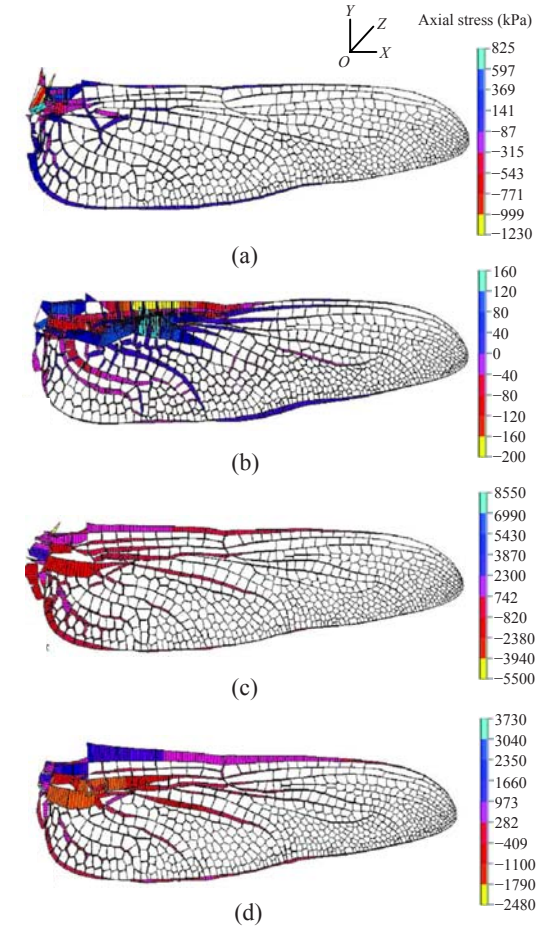

Fig.11 Axial stresses distribution in the veins. (a) Model I; (b) Model II; (c) Model III; (d) Model IV

The pattern of the stress distribution in Model II (Fig.11b) are similar to Model I, but the axial stresses in major veins become even larger close to the wing base and the leading edge, and smaller close to the wing tip and in the posterior vein; in addition, the axial stresses in the secondary veins also become smaller (Table 2).

The axial stresses in the major veins of Model III increase greatly in contrast with those in Models I and II (Table 2). The axial stresses in the veins close to the wing base and the leading edge, and in the posterior vein are much greater, while the stresses in the veins close to the wing tip and in the secondary veins are smaller (Fig.11c).

In contrast with Model III, the distribution of the axial stresses in the veins of Model IV becomes more reasonable (Fig.11d and Table 2); the thicker the vein, the greater the axial stresses in these veins, and vice versa.

Based on the present study, several conclusions can be drawn: (1) When the wing structure is subjected to a uniform out-of-plane transverse loading downwards, the vein sizes in different zones are consistent with their internal forces; (2) The costa, subcosta, median veins, posterior vein are the major veins, forming the main frame of a dragonfly wing and undertaking a large percentage of the external load; (3) The cambered corrugation in the vein-stiffening membrane structure of a dragonfly wing can optimize

Table 2 Axial stresses in the veins of different zones

Vein name	Location	Maximum axial stresses in the vein (kPa)			
		Model I	Model II	Model III	Model IV
Costa	Wing tip	18.07	8.47	239.19	326.74
	Middle of wing	59.00	−14.81	565.66	680.45
	Wing base	−60.84	−180.75	854.95	1133.90
Subcosta	Middle of wing	12.14	9.08	−43.62	−46.98
	Middle of vein	22.91	20.70	−151.16	−143.79
	Wing base	−10.397	−44.78	391.32	218.79
Median vein	Wing tip	−6.67	−7.18	−103.53	−102.68
	Middle of vein	−21.27	−8.48	−270.86	−235.57
	Wing base	27.10	160.16	−208.36	−512.46
Secondary vein	Wing tip	−5.58	−2.17	3.08	−5.43
	Middle of wing	−14.96	−3.40	46.04	3.94
	Wing base	9.84	−4.58	32.90	30.68
Posterior vein	Wing tip	20.46	15.12	69.45	115.10
	Middle of wing	62.78	30.87	51.95	132.41
	Wing base	53.41	−15.05	234.88	288.29

Note: "−" denotes "compressive stress", while "+" before a tensile stress is ignored; for median veins; "wing tip" means the part of veins on the side of the wing tip, and "wing base" means the part of veins on the side of the wing base

the distribution of the internal forces in the wing structure. Similar conclusions can be drawn if a uniformly distributed upward follower loading is exerted on these models (Zhang, 2007).

CONTRIBUTION OF MEMBRANE TO THE FLEXURAL STIFFNESS OF WING STRUCTURE

To evaluate the contribution of the membrane to the flexural stiffness of a dragonfly hind wing, Models II, IV and V were analyzed, respectively. Model V is a 3D model with cambered corrugation, whose out-of-plane coordinates at any point are half of those of Model IV, but its other geometrical parameters and material properties are the same as those of Model IV.

Deflections at three selected points (Fig.12) of these models subject to uniform out-of-plane downward loading on the veins are depicted in Figs.13a~13c, respectively.

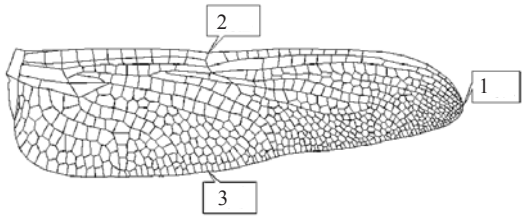

Fig.12 Three selected points on the wing structure

It is shown that the contribution of the membrane to the flexural stiffness of a planar model (Model II) can be ignored, while the contribution of the membrane to the flexural stiffness of 3D models with cambered corrugation (Models IV and V) must be taken into account. With the increase of the arch rise of a 3D model, the flexural stiffness of its pure vein frame becomes stiffer, and the contribution of the membrane to the flexural stiffness of a 3D model becomes more significant.

ROLES OF PTEROSTIGMA AND NODUS IN ALLEVIATING THE WING QUIVERING

In the experiment on the wing and wing pterostigma of a dragonfly *Odonata*, Norberg R.A.(1972) found that the torsion axis of the wing lay ahead of the chordwise centre of the wing mass

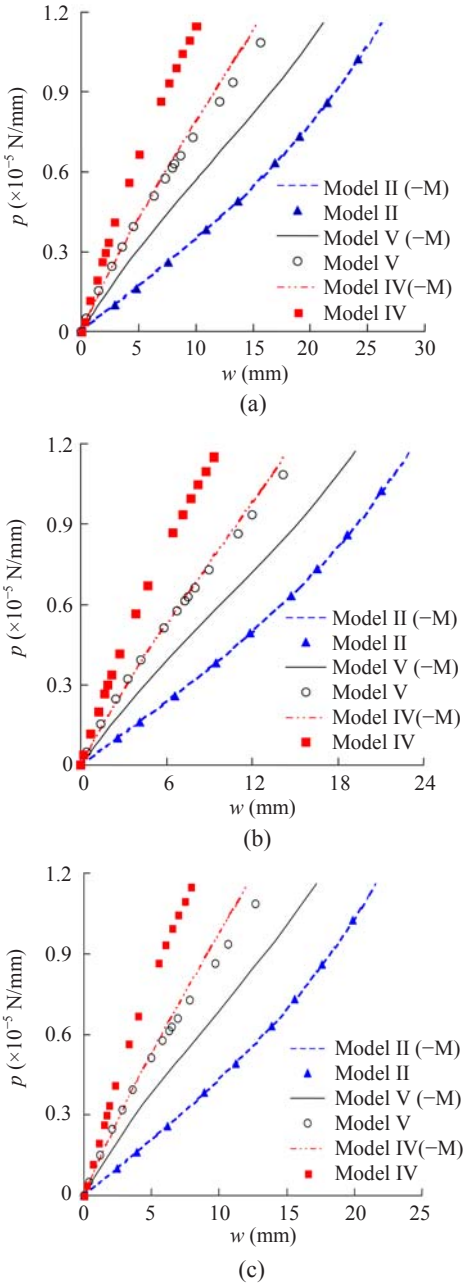

Fig.13 Deflection curves at three selected points of wing models. (a) Position 1; (b) Position 2; (c) Position 3. '−M' in the parentheses means that the contribution of the membrane to the flexural stiffness of the wing structure is ignored in the corresponding model; *p* is line load; *w* is out-of-plane displacement

except at the pterostigma, and that wing without a pterostigma was thus highly susceptible to self-excited coupled flapping and feathering vibrations, making gliding flight above a critical speed impossible and a still lower speed limit set to active flight. By contrast, the pterostigma usually had an

optimal position, which tended to raise these speed limits by causing favourable, inertial, pitching moments during the acceleration phases of wing flapping. The contribution of a pterostigma mass and its enframing veins was 9% of the total wing mass in the forewing of *A. juneea* and 5% in the hind wing (Norberg R.A., 1972). In the present study, the wing pterostigma was replaced by a lumped mass having different values of mass and connecting rigidity with the wing structure to figure out the optimized effect of the pterostigma in alleviating the wing structure quivering effect. In each computational model, the lumped mass was fixed along the leading edge close to the wing tip (Method 1) or connected to the wing model by multiple springs (Method 2) (Fig.14). The pterostigma had a hollow structure (Fig.4), and was filled with viscous body fluid. Considering that the damping effect of the body fluid in the pterostigma on the vibration performance of the wing structure is similar to that of a mass connecting to the wing structure through multiple springs, we adopted an assumption as Method 2, where the relative vibration of the lumped mass to the wing structure was limited in the normal direction of the wing planform. In both methods, the lumped mass was assumed to be 0%, 10% and 20% of the wing mass, respectively.

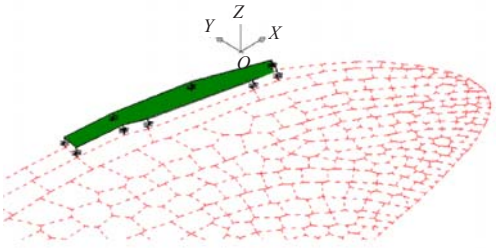

Fig.14 Pterostigma model with multiple springs connecting to the hind wing

The effect of a nodus on the vibration performance of the wing structure was also studied by evaluating respectively the vibrating frequencies of the dragonfly hind wing models with or without a nodus. The nodus was idealized as a hinge, and the structures on two sides of the hinge can rotate relatively, but cannot separate.

Firstly, suppose that the lumped mass is fixed along the leading edge close to the wing tip (Method 1), the fundamental frequencies (1st natural frequency) of each model with different values of lumped mass, and with or without a nodus are presented in Table 3. It is shown that, when 10% of the wing mass is attached, the fundamental frequencies decrease by 10.7%~13.2%, and when 20% of the wing mass is attached, the frequencies decrease by 18.9%~22.4%, thus the lumped mass can lower the fundamental frequencies of these models effectively.

Then suppose that the lumped mass replacing a pterostigma is connected to the wing structure through multiple springs, and it can only vibrate in the normal direction of the wing planform (Method 2). The lumped mass is 0%, 10% and 20% of the wing mass, respectively. The fundamental frequencies of the wing structural models with or without a nodus are shown in Table 3. It demonstrates that, if the lumped mass is 10% of the wing mass, the fundamental frequencies decrease by 16.0%~18.0%; while, if 20% of the wing mass is attached, the frequencies decrease by 23.0%~26.0%.

We can concluded that: (1) The fundamental frequency of a wing model decreases with the increase of the attached mass; (2) With the increase of the arch rise of the cambered corrugation, the fundamental frequency increases rapidly, and the wing structure becomes stiffer; (3) The mass attached to

Table 3 Fundamental frequency of wing models

Model	Fundamental frequency (Hz)				
	$R_{L/W}$=0%	Method 1		Method 2	
		$R_{L/W}$=10%	$R_{L/W}$=20%	$R_{L/W}$=10%	$R_{L/W}$=20%
Model II	42.99 (0.0%)	38.28 (11.0%)	34.82 (19.0%)	35.74 (16.9%)	32.86 (23.6%)
Model II (+N)	42.67 (0.0%)	37.99 (11.0%)	34.55 (19.0%)	35.32 (17.2%)	32.47 (23.9%)
Model V	74.85 (0.0%)	66.81 (10.7%)	60.69 (18.9%)	62.85 (16.0%)	57.64 (23.0%)
Model V (+N)	73.68 (0.0%)	65.60 (11.0%)	59.59 (19.1%)	61.71 (16.2%)	56.59 (23.2%)
Model IV	91.28 (0.0%)	79.24 (13.2%)	70.79 (22.4%)	74.88 (18.0%)	67.58 (26.0%)
Model IV (+N)	91.20 (0.0%)	79.18 (13.2%)	70.75 (22.4%)	74.84 (17.9%)	67.55 (25.9%)

Note: "+N" means that a nodus is included in the corresponding model; the lowered percentages of the fundamental frequencies in models with lumped mass are given in parenthesis; $R_{L/W}$ is percentage of lumped mass to wing mass

the wing structure through multiple springs can lower the fundamental frequency of the wing model more effectively; (4) The effect of a nodus on the fundamental frequency of the wing model can be nearly ignored. These findings are very significant in bionic modeling of a dragonfly wing.

CONCLUSION

The unique vein-stiffening membrane structure of a dragonfly hind wing was studied by using the finite element method. It demonstrates that the venation pattern and the variation of the vein size in different zones in the wing coincide well with the vein internal force under uniformly distributed out-of-plane transverse loading. The cambered corrugation in a wing structure subject to out-of-plane transverse loading leads to the generation of tensile stresses in the membrane of the wing structure, which accordingly improves the wing flexural stiffness effectively. The pterostigma along the wing leading edge close to the wing tip effectively lowers the fundamental frequency of the wing structure, and thus can efficiently alleviate the wing flutter. The nodus exerts little effect on the flexural stiffness and vibrating frequency of the wing structure, whose function still needs further study. It is significant to integrate these superiorities of dragonfly wings into the design of new-style reticulately stiffening thin-walled structural systems and the flapping wings of novel intelligent aircrafts.

ACKNOWLEDGEMENTS

The first author would like to express his gratitude to Profs. Hong Jian and He Li-ping in the Biological Microstructure Lab of Zhejiang University for their warmhearted help in sample tests.

References

Ahmad, S., Irons, B.M., Zienkiewicz, O.C., 1970. Analysis of thick and thin shell structures by curved finite elements. *International Journal for Numerical Methods in Engineering*, **2**(3):419-451. [doi:10.1002/nme.1620020310]

Bradshaw, R., Campbell, D., Gargari, M., Mirmiran, A., Tripeny, P., 2002. Special structures: past, present, and future. *Journal of Structural Engineering ASCE*, **128**(6):691-709. [doi:10.1061/(ASCE)0733-9445(2002)128:6(691)]

Combes, S.A., Daniel, T.L., 2003a. Flexural stiffness in insect wings I. Scaling and the influence of wing venation. *Journal of Experimental Biology*, **206**(17):2979-2987. [doi:10.1242/jeb.00502]

Combes, S.A., Daniel, T.L., 2003b. Flexural stiffness in insect wings II. Spatial distribution and dynamic wing bending. *Journal of Experimental Biology*, **206**(17):2989-2997. [doi:10.1242/jeb.00524]

Cook, R.D., 1981. Concepts and Applications of Finite Element Analysis. John Wiley & Sons, New York.

Dillmann, R., Albiez, J., Gamann, B., Kerscher, T., 2005. Biologically Motivated Control of Walking Machines. *In*: Armada, M.A., Santos, P.G. (Eds.), Climbing and Walking Robots, Springer, Berlin, Heidelberg, p.55-69. [doi:10.1007/3-540-29461-9_4]

Dudley, R., 2000. The Biomechanics of Insect Flight: Form, Function Evolution. Princeton University Press, Princeton.

Ellington, C.P., 1999. The novel aerodynamics of insect flight: applications to micro-air vehicles. *Journal of Experimental Biology*, **202**(23):3439-3448.

Feng, P., Ye, L.P., Teng, J.G., 2007. Large-span woven web structure made of fiber-reinforced polymer. *Journal of Composites for Construction*, **11**(2):110-119. [doi:10.1061/(ASCE)1090-0268(2007)11:2(110)]

Fest, E., Shea, K., Domer, B., Smith, I.F.C., 2003. Adjustable tensegrity structures. *Journal of Structural Engineering ASCE*, **129**(4):515-526. [doi:10.1061/(ASCE)0733-9445(2003)129:4(515)]

Holgate, A., 1990. Aesthetics of thin-walled structures. *Thin-Walled Structures*, **9**(1-4):437-457. [doi:10.1016/0263-8231(90)90057-6]

Ibrahimbegovic, A., 1995. On finite element implementation of geometrically nonlinear reissner's beam theory: three-dimensional curved beam elements. *Computer Methods in Applied Mechanics and Engineering*, **122**(1-2):11-26. [doi:10.1016/0045-7825(95)00724-F]

Isler, H., 1986. Concrete shells and architecture. *Bulletin of the International Association for Shell and Spatial Structures*, **27**(2):39-42.

Izzuddin, B.A., 2005. An enhanced co-rotational approach for large displacement analysis of plates. *International Journal for Numerical Methods in Engineering*, **64**(10):1350-1374. [doi:10.1002/nme.1415]

Kawaguchi, M., Tatemichi, I., Chen, P.S., 1999. Optimum shapes of a cable dome structure. *Engineering Structures*, **21**(8):719-725. [doi:10.1016/S0141-0296(98)00026-1]

Kesel, A.B., Philippi, U., Nachtigall, W., 1998. Biomechanical aspects of the insect wing: an analysis using the finite element method. *Computers in Biology and Medicine*, **28**(4):423-437. [doi:10.1016/S0010-4825(98)00018-3]

Li, Z.X., 2007a. A mixed co-rotational formulation of 2D beam element using vectorial rotational variables. *Communications in Numerical Methods in Engineering*, **23**(1):45-69. [doi:10.1002/cnm.882]

Li, Z.X., 2007b. A co-rotational formulation for 3D beam element using vectorial rotational variables. *Computational Mechanics*, **39**(3):309-322. [doi:10.1007/s00466-006-0029-x]

Li, Z.X., Zheng, Y., 2005. Studies on the Flexible Wings of an Intelligent Aerocraft. *In*: Zhang, G.T., Xing, Q.H. (Eds.), Proceeding of the 1st Annual Academic Conference of Chinese Society of Astronautics. Astronautic Publishing House, Beihai, China, p.730-733 (in Chinese).

Li, Z.X., Vu-Quoc, L., 2007. An efficient co-rotational formulation for curved triangular shell element. *International Journal for Numerical Methods in Engineering*, **72**(9):1029-1062. [doi:10.1002/nme.2064]

Li, Z.X., Izzuddin, B.A., Vu-Quoc, L., 2008. A 9-node co-rotational quadrilateral shell element. *Computational Mechanics*, **42**(6):873-884. [doi:10.1007/s00466-008-0289-8]

Liddell, W.I., Miller, P.W., 1999. Design and construction of the millennium dome. *Structural Engineering International*, **9**(3):172-175. [doi:10.2749/101686699780482023]

Mcrobie, F.A., Lasenby, J., 1999. Simo-Vu Quoc rods using clifford algebra. *International Journal for Numerical Methods in Engineering*, **45**(4):377-398. [doi:10.1002/(SICI)1097-0207(19990610)45:4<377::AID-NME586>3.3.CO;2-G]

Norberg, R.A., 1972. The pterostigma of insect wings an inertial regulator of wing pitch. *Journal of Comparative Physiology A: Neuroethology, Sensory, Neural, and Behavioral Physiology*, **81**(1):9-22. [doi:10.1007/BF00693547]

Norberg, U.M.L., 2002. Structure, form, and function of flight in engineering and the living world. *Journal of Morphology*, **252**(1):52-81. [doi:10.1002/jmor.10013]

Okamoto, M., Yasuda, K., Azuma, A., 1996. Aerodynamic characteristics of the wings and body of a dragonfly. *Journal of Experimental Biology*, **199**(2):281-294.

Schlaich, J., Bergermann, R., Sobek, W., 1994. Air-inflated roof over the Roman amphitheatre at Nimes. *Structural Engineering Review*, **6**(3-4):203-214.

Shapiro, J., 1955. Principles of Helicopter Engineering. Temple Press, London, p.365.

Shen, W., 2006. Studies on New-style Reticulately Stiffening Thin-walled Cantilever by Bionic Modeling of Dragonfly Wings. MS Thesis, Zhejiang University, Hangzhou, p.53-76 (in Chinese).

Shyy, W., Berg, M., Ljungqvist, D., 1999. Flapping and flexible wings for biological and micro air vehicles. *Progress in Aerospace Sciences*, **35**(5):455-505. [doi:10.1016/S0376-0421(98)00016-5]

Simo, J.C., Vu-Quoc, L., 1986. A three-dimensional finite-strain rod model. Part II: computational aspects. *Computer Methods in Applied Mechanics and Engineering*, **58**(1):79-116. [doi:10.1016/0045-7825(86)90079-4]

Somervill, B.A., 2005. The History of the Airplane. The Child's World Inc. Chanhassen, Minnesota.

Sudo, S., Tsuyuki, K., Tani, J., 2000. Wing morphology of some insects. *JSME International Journal*, *Series C: Mechanical Systems*, *Machine Elements and Manufacturing*, **43**(4):895-900.

Sun, Z.J., Zhang, Q.L., 2005. A study on pre-tension measurement of membrane structures. *International Journal of Space Structures*, **20**(2):71-82. [doi:10.1260/0266351054764236]

Sunada, S., Zeng, L.J., Kawachi, K., 1998. The relationship between dragonfly wing structure and torsional deformation. *Journal of Theoretical Biology*, **193**(1):39-45. [doi:10.1006/jtbi.1998.0678]

Tang, C.Y., Tan, K.H., 2004. An interactive mechanical model for shear strength of deep beams. *Journal of Structural Engineering ASCE*, **130**(10):1534-1544. [doi:10.1061/(ASCE)0733-9445(2004)130:10(1534)]

Wootton, R.J., 1990. The mechanical design of insect wings. *Scientific American*, **263**(5):114-120.

Wootton, R.J., Kukalová-Peck, J., Newman, D.J.S., Muzón, J., 1998. Smart engineering in the Mid-Carboniferous: How well could *Palaeozoic* dragonflies fly? *Science*, **282**(5389): 749-751. [doi:10.1126/science.282.5389.749]

Zeng, L.J., Matsumoto, H., Kawachi, K., 1996. Simultaneous measurement of the shape and thickness of a dragonfly wing. *Measurement Science & Technology*, **7**(12):1728-1732. [doi:10.1088/0957-0233/7/12/006]

Zhang, G., 2007. Studies on New-style Spatial Cantilever Structures by Bionic Modeling of Dragonfly Wings. MS Thesis, Zhejiang University, Hangzhou, p.63-69 (in Chinese).

Zhang, Q.L., Zhang, L., 2000. Three kinds of shape finding problems and their solutions for membrane structures. *Journal of Building Structures*, **21**(5):33-40 (in Chinese).

Zhang, Q.L., Chen, L.X., Luo, X.Q., Yang, Z.L., 2007. Equivalent transform from the force-densities of cable nets to the stresses of membrane elements. *Structural Engineering and Mechanics*, **26**(4):479-482.

Zhang, Y.X., Cheung, Y.K., 2003. A refined non-linear non-conforming triangular plate/shell element. *International Journal for Numerical Methods in Engineering*, **56**(15):2387-2408. [doi:10.1002/nme.667]

Zhang, Y.X., Kim, K.S., 2005. Linear and geometrically nonlinear analysis of plates and shells by a new refined non-conforming triangular plate/shell element. *Computational Mechanics*, **36**(5):331-342. [doi:10.1007/s00466-004-0625-6]